MEDICAL SCIENCE MONITOR

ANIMAL STUDY

e-ISSN 1643-3750
© Med Sci Monit, 2017; 23: 3404-3411
DOI: 10.12659/MSM.902227

Received: 2016.11.04
Accepted: 2016.12.20
Published: 2017.07.13

The Effects and Possible Mechanisms of Puerarin to Treat Uterine Fibrosis Induced by Ischemia-Reperfusion Injury in Rats

Authors' Contribution:
Study Design A
Data Collection B
Statistical Analysis C
Data Interpretation D
Manuscript Preparation E
Literature Search F
Funds Collection G

ADEF 1 Lin Lin
ABCD 2 Yi He
BCD 3 Jiashu Zhang
AEF 3 Qi Liu
ACDF 1 Lixia Wang

1 Department of Gynaecology and Obstetrics, The Second Affiliated Hospital of Dalian Medical University, Dalian, Liaoning, P.R. China
2 Department of Urology, The Second Affiliated Hospital of Dalian Medical University, Dalian, Liaoning, P.R. China
3 College of Pharmacy, Dalian Medical University, Dalian, Liaoning, P.R. China

Corresponding Authors: Lixia Wang, e-mail: wanglixia691130@163.com, Qi Liu, e-mail: llaqiidl@163.com
Source of support: Departmental sources

Background: Tissues fibrosis is caused by ischemia-reperfusion injury (IRI) and results in organ dysfunction. In this study, we aimed to investigate whether fibrosis occurs after uterine ischemia-reperfusion injury, and to investigate the effects of puerarin (Pur) on the fibrosis process in rats.

Material/Methods: Twenty-four female Wistar rats were randomly divided into three groups (8 in each group): the control group rats only received operation without uterine ischemic, the IRI group and the IRI + Pur group rats received 30-minutes ischemia and 2-weeks of reperfusion. Pur was orally administered at the onset of reperfusion. Picrosirius red staining was used to assess uterine fibrosis. Immunohistochemistry was used to detect the expression levels of transforming growth factor (TGF)-β and α-smooth muscle actin (α-SMA). Western blotting was used to evaluate the expression of chymase, TGF-β, α-SMA, and the activity of the Wnt/β-catenin pathway.

Results: Uterine fibrosis in the IRI+Pur group was significantly decreased compared with the IRI group. In addition, immunohistochemistry reveals that TGF-β and α-SMA were decreased in the IRI+Pur group compared with the IRI group. Western blotting results showed that Pur significantly suppresses the increase in chymase, α-SMA, TGF-β, and β-catenin expression levels induced by IRI.

Conclusions: The results indicated that IRI could induce uterine fibrosis and that Pur had an improvement effect on IRI-induced uterine fibrosis by downregulating the activity of mast cell chymase, TGF-β, α-SMA, and the Wnt/β-catenin pathway.

MeSH Keywords: Fibrosis • Mast Cells • Pueraria • Uterine Artery

Full-text PDF: http://www.medscimonit.com/abstract/index/idArt/902227

2383 — 5 32

This work is licensed under Creative Common Attribution-NonCommercial-NoDerivatives 4.0 International (CC BY-NC-ND 4.0)

Indexed in: [Current Contents/Clinical Medicine] [SCI Expanded] [ISI Alerting System] [ISI Journals Master List] [Index Medicus/MEDLINE] [EMBASE/Excerpta Medica] [Chemical Abstracts/CAS] [Index Copernicus]

Background

The phenomenon of temporary ischemia of the uterus is common in gynecology and obstetrics [1,2]. However, there are few studies on the pathophysiologic changes and treatment of uterine ischemia and reperfusion injury (IRI).

Fibrosis, which is mechanistically characterized by myofibroblast accumulation, collagen deposition, extracellular matrix (ECM) remodeling [3,4], and increased tissue stiffness, produces a highly collagenized tissue that impairs organ function [5,6]. Uterine fibrosis may impair fertility [7] and promote miscarriage [8] by reducing uterine elasticity and compliance, which is important for normal pregnancy.

As previously reported, IRI induces tissue fibrosis in different organs [9,10]. However, the role of fibrosis in the uterus after IRI is poorly understood. Therefore, we researched whether uterine healing and remodeling following ischemic injury, occurred with characteristic myofibroblast trans-differentiation and scar formation. It has been reported that mast cells could potentially promote fibrosis, which is intricately linked with the pleiotropic cytokine transforming growth factor (TGF)-β. TGF-β has important physiological roles in initiation and control of fibrosis [11,12]. In addition, mast cells produce and activate TGF-β, through the production of chymases [13–15]. Also, TGF-β is a potent mast cell chemoattractant [16]. It is reported that the Wnt/β-catenin signaling pathway is essential for fibrosis induced by TGF-β [17,18]. The Wnt/β-catenin/TGF-β signaling pathway is a key mediator of fibroblast activation [19,20] and drives the aberrant synthesis of the extracellular matrix in fibrotic diseases.

Puerarin (Pur) is a bioactive isoflavone glucoside derived from the traditional Chinese medicine pueraria [21,22]. Evidence suggests that Pur has many anti-inflammatory and anti-fibrosis properties and has a positive effect on IRI [23–25]. However, little is known about the role and detailed mechanism of Pur in the fibrosis process induced by uterine ischemic damage.

The aim of this present study was to observe the effects of Pur on the signaling transmission of fibrosis mediated by the Wnt/β-catenin/TGF-β signaling pathway after uterine ischemic damage.

Material and Methods

Chemicals

Pur was purchased from Shanxi Bosen BioPharmaceutical Co., Ltd. (Xi'an, China). All other chemicals used in this study were analytical grade and commercially available.

Animals

Female Wistar rats (180±20 g) were purchased from the Experimental Animal Center of Dalian Medical University (Dalian, China). Rats were allowed access to water and food ad libitum, but fasted overnight with water available before surgery.

Ethical approval

All applicable international, national, and/or institutional guidelines for the care and use of animals were followed. All animal experiments were approved by the ethics committee of Dalian Medical University and performed in accordance with the institutional guidelines.

Experimental protocol

Since the thickness of the endometrium varies during different sexual cycles, all rats in our study were synchronized in the estrous cycle, which was judged as described by Marcondes et al. [26]. The animals were randomly divided into three experimental groups:

Sham group (n=8) received only the operation without uterine ischemic procedure, and had daily administration of normal saline.

IRI group (n=8) had celiac artery ligatured for 30 minutes, and had daily administration of normal saline.

IRI+Pur group (n=8) had celiac artery ligatured for 30 minutes and Pur was administered at the onset of reperfusion (100 mg/kg intraperitoneally once daily).

Uterine ischemia-reperfusion surgery

The method of model construction was a standard method [27]. The surgery was conducted by the same surgeon. Immediately after the animals were anesthetized by 10% chloral hydrate (3–5 mL/kg, intraperitoneally), the skin was prepped, and the mouse placed on a homeothermic blanket of a homeothermic monitor system and covered by sterile gauze. The body temperature was monitored through a rectal probe and controlled in the range of 36.5–37°C. Surgery started only after: 1) the body temperature was stabilized at the set-point, and 2) the mouse was in deep anesthesia and thus did not respond to pain induced by toe pinch. The operation was performed after preoperative fasting for 8 hours. It consisted of making about a 4 cm long incision at the middle of the abdomen, poking the abdominal organs, carefully separating the celiac artery, clamping the celiac artery with micro-aneurysm clips to achieve ischemia; complete ischemia was indicated by a color

This work is licensed under Creative Common Attribution-NonCommercial-NoDerivatives 4.0 International (CC BY-NC-ND 4.0)

Indexed in: [Current Contents/Clinical Medicine] [SCI Expanded] [ISI Alerting System] [ISI Journals Master List] [Index Medicus/MEDLINE] [EMBASE/Excerpta Medica] [Chemical Abstracts/CAS] [Index Copernicus]

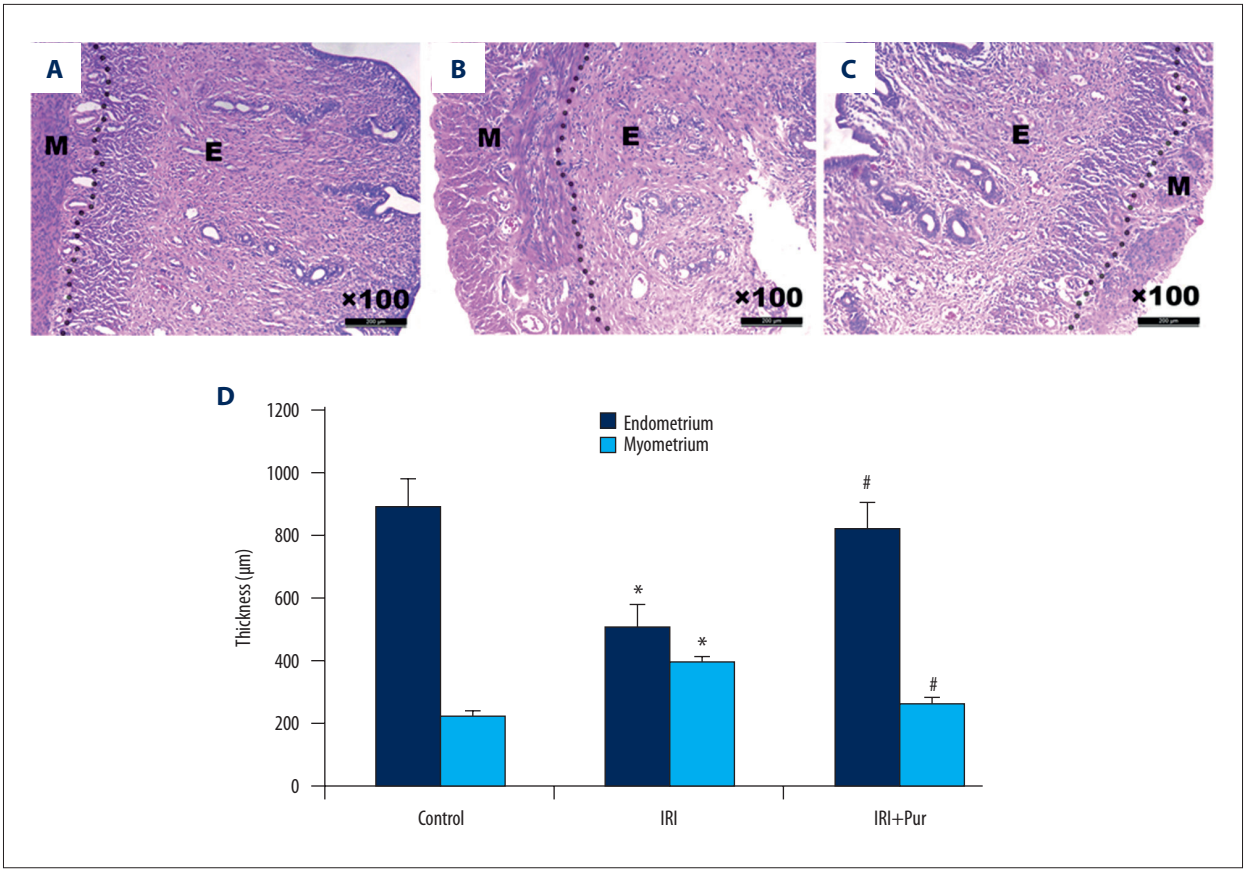

Figure 1. The change in uterine photomicrographs of IRI rats. The uterine are stained with H&E. (**A–C**) 14 days following IRI in rats. The endometrium (E) and myometrium (M) are visualized and quantified at their junction (dotted lines). Representative sections from uterine tissue of a control rat (**A**), IRI rat (**B**), and Pur-treated rat (**C**). H&E, magnification ×100. (**D**) Comparison of the endometrium or myometrium thickness of groups. Data are expressed as mean ±SD. (* $p<0.01$ versus control group; # $p<0.01$ versus IRI group; n=8)

change of the uterine tissue from bright red to dark purple. After the ischemia operation, the micro-aneurysm clips were released at 30 minutes to start the reperfusion, which was indicated by the change of uterine tissue color to red. The closer of the muscle layer of the incision was followed by the closure of the skin wound. After the surgery, the rats had free food and water.

Morphological changes

At two weeks post-reperfusion, the rats were sacrificed. The uteruses of rats were removed, and fixed in 10% (v/v) neutral formalin and processed by standard histological techniques. The uterine tissue was stained with hematoxylin and eosin (H & E) and Picrosirius red staining. Then the uterine tissue was examined for morphological changes. The uterine tissue was also used to determinate the expression of protein of chymase, TGF-β, β-catenin, and α-SMA by Western blot analysis and immunohistochemical staining. The thickness of the endometrium and myometrium were measured with image-processing software (Image-ProPlus 6.0) using photos taking from slides. The thickness and morphology were evaluated and compared between the groups [28].

Western blot analysis

According to the manufacturer's instructions, proteins were extracted from rat uterine tissue using a protein extraction kit (KeyGen Biotech, Nanjing, China), then measured by bicinchoninic acid (BCA) (Solarbio, Beijing, China), with bovine serum albumin as the standard. Proteins were resuspended in electrophoresis sample buffer and separated by electrophoresis on pre-cast 10% SDS-polyacrylamide gels (Bio-Rad, Hercules, CA, USA), followed by an electro-transfer to PVDF membranes (Millipore, Bedford, MA, USA). Blocking of the membranes was done using 5% non-fat milk in Tris-buffered saline with 0.1% Tween-20 (TBST) for 1.5 hours at 37°C. β-actin served as the loading control. Membranes were incubated overnight at 4°C with a polyclonal antibody for chymase (1: 1,000), TGF-β (1: 1,000), β-catenin (1: 1,000), or α-SMA(1: 1,000) (Beijing

This work is licensed under Creative Common Attribution-NonCommercial-NoDerivatives 4.0 International (CC BY-NC-ND 4.0)

Indexed in: [Current Contents/Clinical Medicine] [SCI Expanded] [ISI Alerting System] [ISI Journals Master List] [Index Medicus/MEDLINE] [EMBASE/Excerpta Medica] [Chemical Abstracts/CAS] [Index Copernicus]

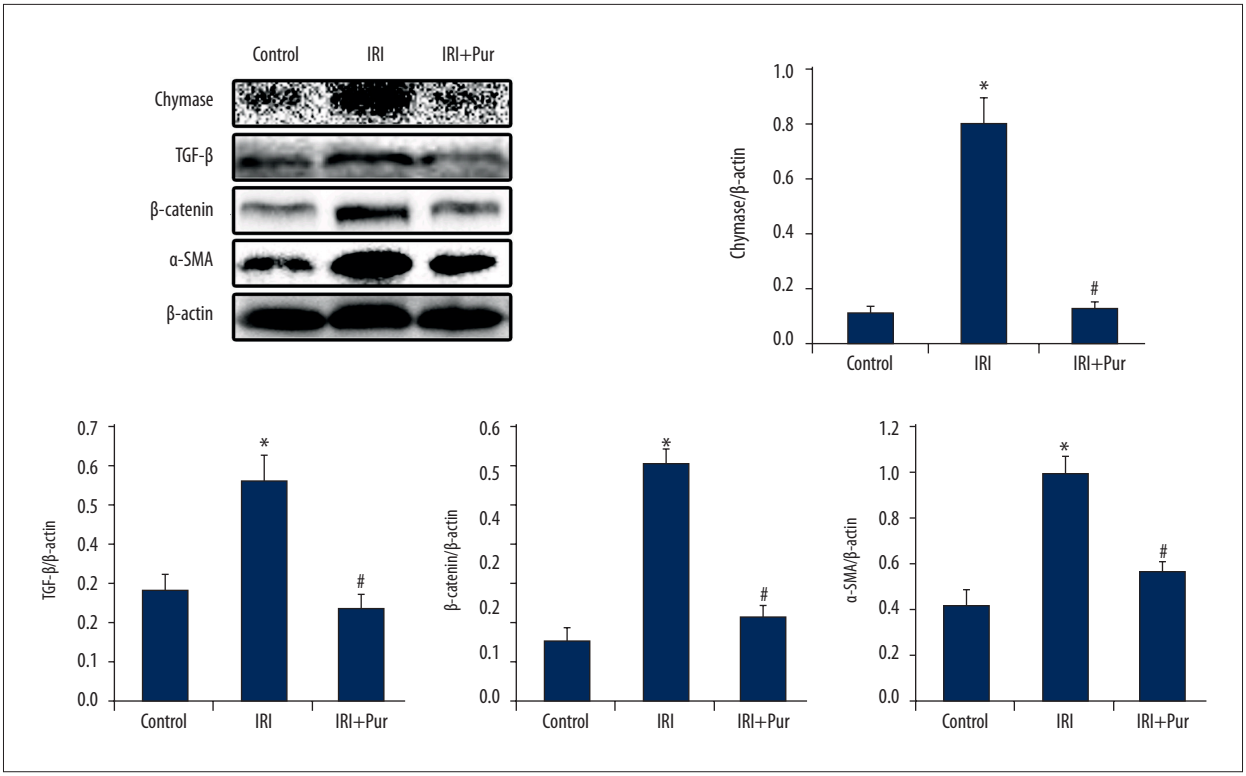

Figure 2. Effect of Pur on the protein expression of chymase, TGF-β, β-catenin, and α-SMA in IRI rat uterine tissue. The bar graph shows the relative expression ratio of each protein calculated after normalization by β-actin. Data are expressed as mean ±SD. (* p<0.01 versus control group; # p<0.01 versus IRI group; n=8).

Biosynthesis Biotechnology, China), and with a 1: 1,000 dilution of monoclonal antibody for β-actin (Beyotime, China), then wash with TBST. The blots were then incubated with secondary antibodies, washed with TBST, and exposed to enhanced chemiluminescence-plus reagents (ECL) from Beyotime Institute of Biotechnology (Haimen, China). The emitted light was documented with a BioSpectrum-410 multispectral imaging system with a Chemi HR camera 410 (Bio-Rad, Hercules, CA, USA). Protein bands are visualized and photographed under transmitted ultraviolet light for semi-quantitative measurements.

Immunohistochemical staining

Histological sections of rat uterine tissue (4 μm thick) were mounted on poly-L-lysine-coated slides. Slides were deparaffinized in xylene and rehydrated in graded alcohols. Sections are pretreated with citrate buffer (0.01 mol/L citric acid, pH 6.0) for 20 minutes at 95°C. Then at room temperature they are immersed in PBS containing 3% H_2O_2 for 10 minutes. After treatment, sections were exposed to 10% normal goat serum in PBS for 30 minutes at room temperature, and the tissue sections were incubated at 4°C overnight with rabbit polyclonal anti-TGF-β (1: 100) and α-SMA (dilution 1: 100). Then sections were rinsed with PBS, incubated with biotinylated goat anti-rabbit IgG for 20 minutes at room temperature and treated with 3,30-diaminobenzidine chromogen for five minutes at room temperature. Finally, sections are counterstained with hematoxylin for two minutes. For semi-quantitative analysis of the protein expression of TGF-β and α-SMA, the sections were measured using a quantitative digital image analysis system (Image-Pro Plus 6.0) [29].

Collagen quantification

Picrosirius red staining was performed with serially sectioned tissues. Paraffin-embedded tissues were deparaffinized in xylene, rehydrated in graded alcohols, and then incubated in 0.1% Picrosirius red solution for one hour at room temperature. Finally, sections were counterstained with hematoxylin for two minutes. The sections were studied under a light microscope at different magnifications. For semi-quantitative analysis of uterine fibrosis, the sections are measured using a quantitative digital image analysis system (Image-Pro Plus 6.0) [30].

Data analysis

Statistical analysis was computed using the SPSS 13.0 software. Group data were expressed as the mean ± standard deviation (SD). One-way analysis of variance (ANOVA) following Dunnett's test was used to compare statistically significant

This work is licensed under Creative Common Attribution-NonCommercial-NoDerivatives 4.0 International (CC BY-NC-ND 4.0)

Indexed in: [Current Contents/Clinical Medicine] [SCI Expanded] [ISI Alerting System] [ISI Journals Master List] [Index Medicus/MEDLINE] [EMBASE/Excerpta Medica] [Chemical Abstracts/CAS] [Index Copernicus]

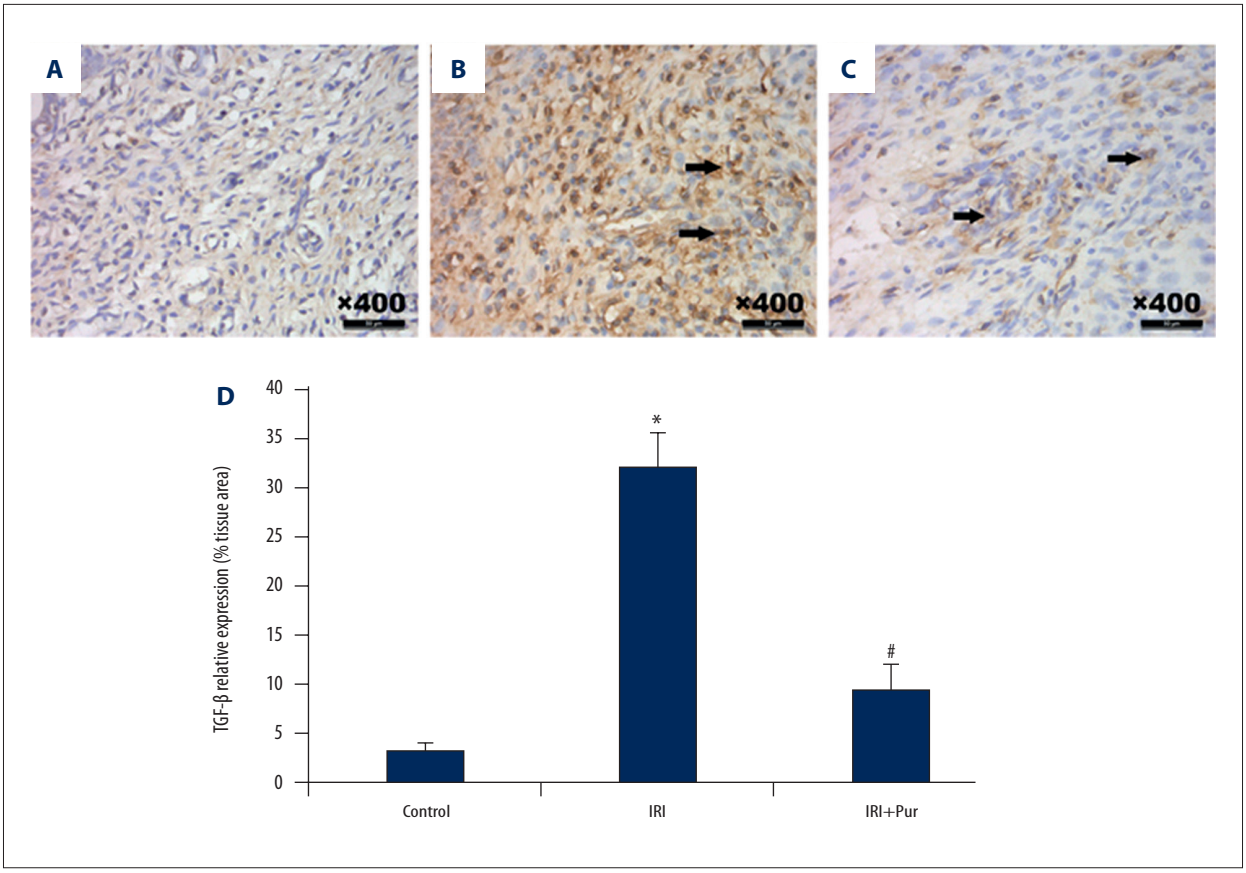

Figure 3. Effect of Pur on the protein expression of TGF-β in IRI rat uterine tissue. IHC with specific TGF-β antibody detects cellular expression pattern in the uterine tissues 14 days following IRI in rats. The positive cells (arrows) are stained brown. Representative sections from uterine tissue of a control rat (**A**), IRI rat (**B**), and Pur-treated rat (**C**). Magnification ×400. (**D**) Comparison of the relative areas stained positively for TGF-β of groups. Data are expressed as mean ±SD. (* $p<0.01$ versus control group; # $p<0.01$ versus IRI group; n=8).

differences in the data between two sets. In all statistical analyses, the level of significance is established as $p<0.05$ or $p<0.01$.

Results

Histological examinations

H&E staining of uterine tissues showed that the muscle fibers were arranged in disorder and uterine tissue from IRI rats exhibit a thinner layer of endometrium ($p<0.01$), a thicker layer of myometrium ($p < 0.01$) than those in the control group. However, the pathology of IRI uterine tissue was reversed significantly by Pur treatment ($p<0.01$, Figure 1).

Pur reduces mast cell chymase production

Since mast cell chymases play an essential role in the fibrosis process, their production level in the case of Pur treatment is of interest. To investigate this, rat uterine tissue was immediately acquired after sacrifice for Western blot analysis. The results of Western blot analysis showed that protein expression of chymase was increased significantly compared with the control group ($p<0.01$, Figure 2). After treatment with Pur for the IRI rats, protein expressions in the uterine tissue was significantly decreased compared with the IRI group ($p<0.01$, Figure 2).

Pur inhibits activity of TGF-β and WNT/β-catenin pathway

TGF-β is a pro-fibrotic cytokine which induces macrophages and proliferation of fibroblasts through the induction of other growth factors. It has been reported that the Wnt/β-catenin signaling pathway is essential for fibrosis induced by TGF-β. Our Western blot analysis of TGF-β ($p<0.01$) and β-catenin ($p<0.01$) showed that increased expression of both proteins was evident in the IRI group, whereas treatment with Pur, showed a significant decrease ($p<0.01$, Figure 2).

The immunohistochemistry results were similar to the aforementioned results. The protein expression of TGF-β in the

This work is licensed under Creative Common Attribution-NonCommercial-NoDerivatives 4.0 International (CC BY-NC-ND 4.0)

Indexed in: [Current Contents/Clinical Medicine] [SCI Expanded] [ISI Alerting System] [ISI Journals Master List] [Index Medicus/MEDLINE] [EMBASE/Excerpta Medica] [Chemical Abstracts/CAS] [Index Copernicus]

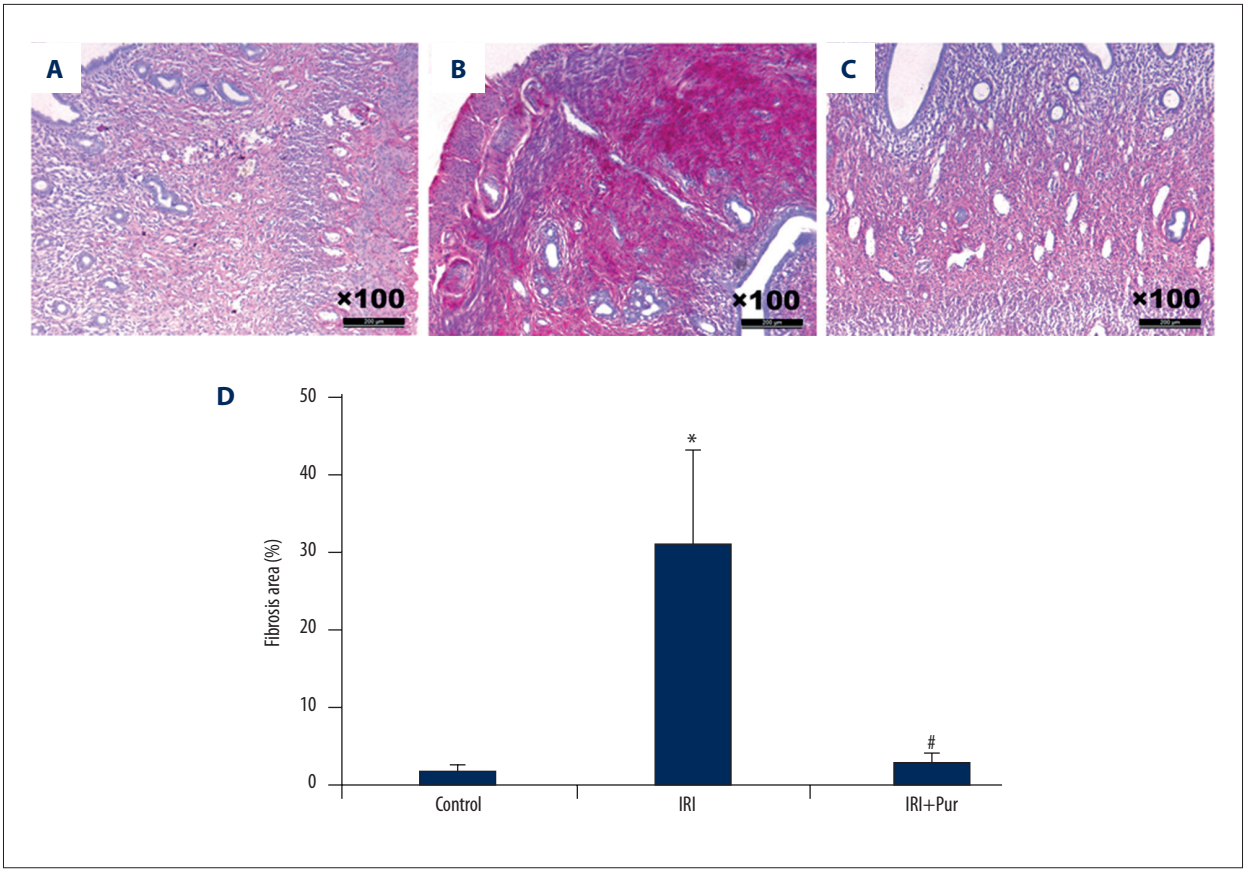

Figure 4. Effect of Pur on the collagen accumulation in IRI rat uterine tissue. The uterine tissues are Picrosirius red stained (**A–C**) 14 days following IRI in rats. Representative sections from uterine tissue of a control rat (**A**), IRI rat (**B**), and Pur-treated rat (**C**). Picrosirius red staining, magnification ×100. (**D**) Comparison of the percent of fibrosis of each group. Data are expressed as mean ±SD. (* $p<0.01$ versus control group; # $p<0.01$ versus IRI group; n=8).

uterine tissue of the IRI group was significantly increased compared with the control group ($p<0.01$). However, after treatment with Pur in the IRI group, protein expression of TGF-β was significantly decreased compared with the IRI group ($p<0.01$, Figure 3).

Pur reduces collagen accumulation in the IRI group uterine tissue.

Picrosirius red staining suggested significantly greater collagen content in the IRI group compared with the control groups ($p<0.01$), and the content was decreased after Pur treatment ($p<0.01$, Figure 4). Moreover, the immunohistochemistry (Figure 5) and Western blot (Figure 2) results showed that the expression level of α-SMA in the uterine tissue of the IRI group was increased significantly compared with the control group ($p<0.01$). However, the protein expression of α-SMA after Pur treatment was significantly decreased compared with the IRI group ($p<0.01$).

Discussion

Tissue fibrosis is epidemiologically associated with the subsequent development of tissue ischemic-reperfusions injury (IRI) in multiple organ systems, leading to dysfunction [19]. However, the role of fibrosis induced by IRI in the uterus is poorly reported. The fibrosis process is mechanistically characterized by myofibroblast accumulation, collagen deposition, extracellular matrix (ECM) remodeling, and increased tissue stiffness, so that highly collagenized tissue impairs organ function by reducing tissue elasticity and compliance. As we all know, uterine elasticity and compliance is important for normal pregnancy. Recently, it has been proposed that smooth muscle cells respond to injury or ischemia with increased cell proliferation and production of extracellular matrix [31]. We hypothesized that uterine IRI induced fibrosis, which reduced uterine elasticity and compliance, thus impairing fertility and promoting miscarriage. Therefore, it is important to suppress the fibrosis process that is induced by IRI. In our study, H&E staining showed that the muscular layer in uterine tissue in the IRI group was arranged in disorder with fracture, a thinner

This work is licensed under Creative Common Attribution-NonCommercial-NoDerivatives 4.0 International (CC BY-NC-ND 4.0)

Indexed in: [Current Contents/Clinical Medicine] [SCI Expanded] [ISI Alerting System] [ISI Journals Master List] [Index Medicus/MEDLINE] [EMBASE/Excerpta Medica] [Chemical Abstracts/CAS] [Index Copernicus]

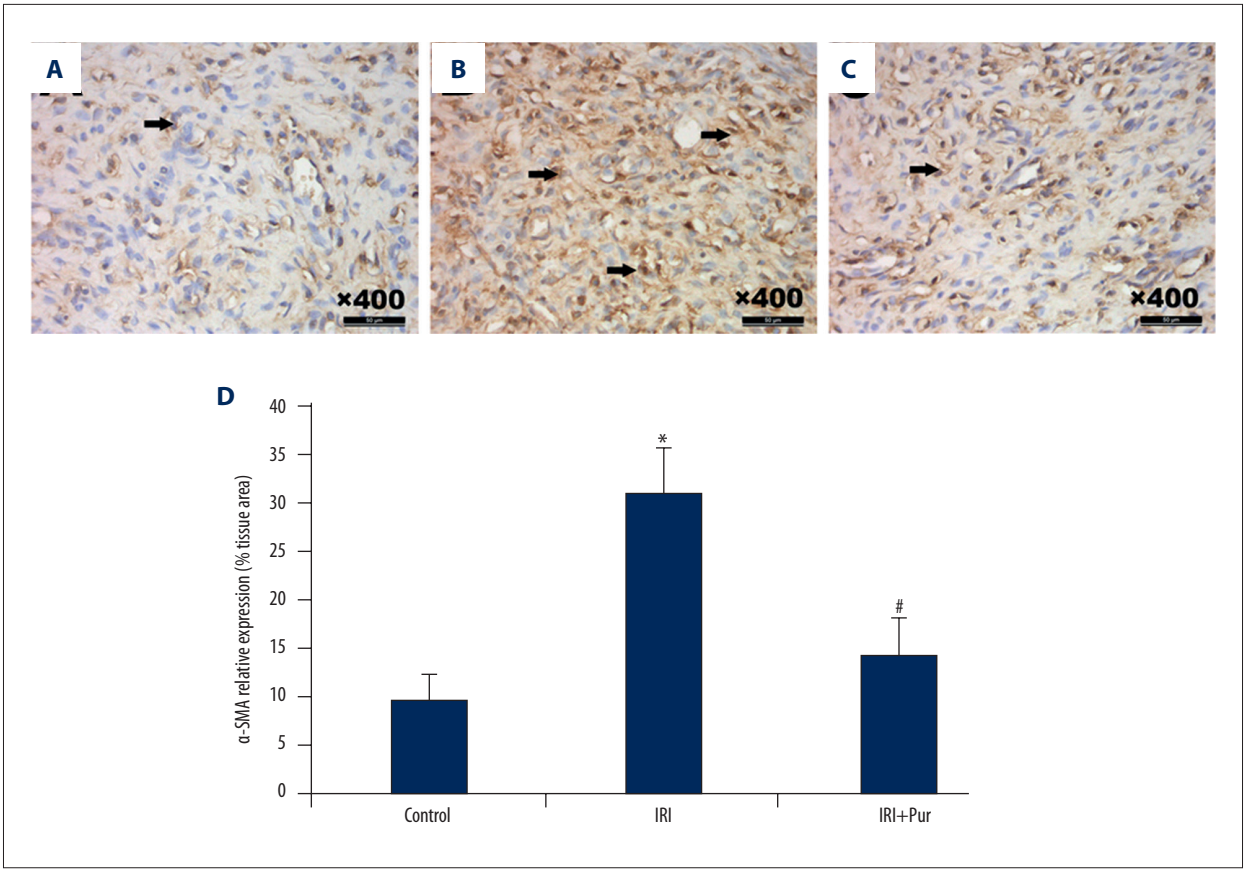

Figure 5. The effect of Pur on the protein expression of α-SMA in IRI rat uterine tissue. IHC with specific α-SMA antibody detects cellular expression pattern in the uterine tissues 14 days following IRI in rats. The positive cells (arrows) stain brown. Representative sections from uterine tissue of a control rat (**A**), IRI rat (**B**), and Pur-treated rat (**C**). Magnification ×400. (D) Comparison of the relative areas stained positively for α-SMA of groups. Data are expressed as mean ±SD. (* $p<0.01$ versus control group; # $p<0.01$ versus IRI group; n=8).

layer of endometrium, and a thicker layer of myometrium compared with the control group. Picrosirius red staining suggested significantly greater collagen content in the IRI group compared with the control group, and Western blots showed that the expression level of α-SMA, known as marker of myofibroblast, in the IRI group was significantly higher than in the control group. However, after treatment with Pur, these changes were significantly suppressed, which indicated that fibrosis was induced in uterine tissue after IRI, which could then be improved by Pur treatment.

Experimental studies have shown that mast cell numbers and staining intensity are linked with increased TGF-β production and interstitial fibrosis [32]. TGF-β, which can be stimulated by mast cell chymase activation, is a ubiquitous pro-fibrotic cytokine with variable functions in the processes of cell differentiation, cell proliferation [19,20]. It has been reported that TGF-β upregulates the synthesis of many extracellular matrix proteins that are associated with tissue fibrosis [11,12]. TGF-β transmits its signals through several intracellular signaling molecules, and it has been reported that the Wnt/β-catenin signaling pathway is essential for fibrosis induced by TGF-β. Therefore, inhibition of the Wnt/β-catenin/TGF-β signaling pathway may play a role in attenuating fibrosis after IRI. In this study, increased expression levels of TGF-β in the uterine tissue of IRI rats compared to the control group were observed. Upon treatment of IRI rats with Pur, a significant decrease in the expression level of TGF-β was observed. In IRI rats, increased expression levels of chymase, β-catenin, and α-SMA were observed, and these were also reduced after Pur treatment. Therefore, the anti-fibrotic effect of Pur might be due to its ability to interact with mast cell chymase and the Wnt/β-catenin/TGF-β signaling pathway. Thus, after IRI, mast cells are activated and produce chymases. Then the chymases stimulate TGF-β production to activate the Wnt/β-catenin pathway in fibroblasts, which can result in increased collagen deposition. However, Pur treatment could also suppress the pro-fibrotic process thus inhibiting the fibrosis induced by IRI. Evidence for the anti-fibrotic role for Pur appears to be strong as supported by our experimental data as discussed.

This work is licensed under Creative Common Attribution-NonCommercial-NoDerivatives 4.0 International (CC BY-NC-ND 4.0)

Indexed in: [Current Contents/Clinical Medicine] [SCI Expanded] [ISI Alerting System] [ISI Journals Master List] [Index Medicus/MEDLINE] [EMBASE/Excerpta Medica] [Chemical Abstracts/CAS] [Index Copernicus]

Conclusions

In summary, exposure of rats to IRI leads to uterine fibrosis. Similar to the pathogenesis of IRI, the progression of fibrosis is mediated by multiple cell signaling factors. The decreased expression levels of mast cell chymase, TGF-β, and other proteins involved in the Wnt/β-catenin signaling pathway after Pur treatment indicated that Pur regulates fibrosis, which is aberrant in IRI-induced tissues. The results of this study demonstrated uterine fibrosis after IRI and the anti-fibrotic effect of Pur. Therefore, Pur can be considered a candidate drug for the treatment of uterine fibrosis induced by IRI.

References:

1. Gosden, Roger G: Ovary and uterus transplantation. Reproduction, 2008; 136: 671–80
2. Ly A, Mills AM, McKenney JK et al: Atypical Leiomyomas of the Uterus: A Clinicopathologic Study of 51 Cases. Am J Surg Pathol, 2013; 37: 643–49
3. Xie T, Liang J, Liu N et al: Transcription factor TBX4 regulates myofibroblast accumulation and lung fibrosis. J Clin Invest, 2016; 126: 3063–79
4. Rezvani M, Español-Suñer R, Malato Y et al: *In vivo* hepatic reprogramming of myofibroblasts with AAV vectors as a therapeutic strategy for liver fibrosis. Cell Stem Cell, 2016; 18: 809–16
5. Nishiyama O, Tohda Y: Obstructive lung function in idiopathic pulmonary fibrosis. Chron Respir Dis, 2016; 3: 206
6. Toki D, Inui M, Ishida H et al: Interstitial fibrosis is the critical determinant of impaired renal function in transplant glomerulopathy. Nephrology (Carlton), 2016; 21: 20–25
7. Alawadhi F, Du H, Cakmak H, Taylor HS: Bone marrow-derived stem cell (BMDSC) transplantation improves fertility in a murine model of asherman's syndrome. PLoS One, 2014; 9: e96662
8. Li J, Du S, Sheng X et al: MicroRNA-29b inhibits endometrial fibrosis by regulating the Sp1-TGF-β1/Smad-CTGF axis in a rat model. Reprod Sci, 2016; 23: 386–94
9. Colombaro V, Jadot I, Declèves AE et al: Lack of hyaluronidases exacerbates renal post-ischemic injury, inflammation, and fibrosis. Kidney Int, 2015; 88: 61–71
10. Gao HC, Zhao H, Zhang WQ: The role of the Rho/Rock signaling pathway in the pathogenesis of acute ischemic myocardial fibrosis in rat models. Exp Ther Med, 2013; 5: 1123–28
11. Meng XM, Nikolic-Paterson DJ, Lan HY: TGF-β: the master regulator of fibrosis. Nat Rev Nephrol, 2016: 12: 325–38
12. Wang S, Meng XM, Ng YY et al: TGF-β/Smad3 signalling regulates the transition of bone marrow-derived macrophages into myofibroblasts during tissue fibrosis. Oncotarget, 2016; 7: 8809–22
13. Gordon JR, Galli SJ: Promotion of mouse fibroblast collagen gene expression by mast cells stimulated via the Fc epsilon RI. Role for mast cell-derived transforming growth factor beta and tumor necrosis factor alpha. J Exp Med, 1994; 180: 2027–37
14. Pennington DW, Lopez AR, Thomas PS et al: Dog mastocytoma cells produce transforming growth factor beta 1. J Clin Invest, 1992; 90: 35–41
15. Lindstedt KA, Wang Y, Shiota N et al: Activation of paracrine TGF-beta1 signaling upon stimulation and degranulation of rat serosal mast cells: A novel function for chymase. FASEB J, 2001; 15: 1377–88
16. Gruber BL, Marchese MJ, Kew RR: Transforming growth factor-beta 1 mediates mast cell chemotaxis. J Immunol, 1994; 152: 5860–67
17. Akhmetshina A, Palumbo K, Dees C et al: Activation of canonical Wnt signalling is required for TGF-β-mediated fibrosis. Nat Commun, 2011; 3: 735
18. Blyszczuk P, Müller-Edenborn B, Valenta T et al: Transforming growth factor-β-dependent Wnt secretion controls myofibroblast formation and myocardial fibrosis progression in experimental autoimmune myocarditis. Eur Heart J, 2016 [Epub ahead of print]
19. Chen D, Jarrell A, Guol C: Dermal β-catenin activity in response to epidermal Wnt ligands is required for fibroblast proliferation and hair follicle initiation. Development, 2012; 139: 1522–33
20. Zerr P, Palumbo-Zerr K, Huang J: Sirt1 regulates canonical TGF-beta signalling to control fibroblast activation and tissue fibrosis. Ann Rheum Dis, 2016; 75: 226–33
21. Zhang Z, Lam TN, Zuo Z: Radix puerariae: An overview of its chemistry, pharmacology, pharmacokinetics, and clinical use. J Clin Pharmacol, 2013; 53: 787–811
22. Cherdshewasart W, Subtang S, Dahlan W: Major isoflavonoid contents of the phytoestrogen rich-herb *Pueraria mirifica* in comparison with *Pueraria lobata*. J Pharm Biomed Anal, 2007; 43: 428–34
23. Wang S, Shi XL, Feng M et al: Puerarin protects against CCl4-induced liver fibrosis in mice: Possible role of PARP-1 inhibition. Int Immunopharmacol, 2016; 38: 238–45
24. Yuan Y, Zhou H, Wu QQ et al: Puerarin attenuates the inflammatory response and apoptosis in LPS-stimulated cardiomyocytes. Exp Ther Med, 2016; 11: 415–20
25. Liu S, Zhang C, Shi Q et al: Puerarin blocks the signaling transmission mediated by P2X3 in SG and DRG to relieve myocardial ischemic damage. Brain Res Bull, 2014; 101: 57–63
26. Marcondes FK, Bianchi FJ, Tanno AP: Determination of the estrous cycle phases of rats: Some helpful considerations. Braz J Biol, 2002; 62: 609–14
27. Sahin S, Ozakpinar OB, Ak K et al: The protective effects of tacrolimus on rat uteri exposed to ischemia-reperfusion injury: A biochemical and histopathologic evaluation. Fertil Steril, 2014; 101: 1176–82
28. Zhao J, Zhang Q, Wang YG, Li YP:. Uterine infusion with bone marrow mesenchymal stem cells improves endometrium thickness in a rat model of thin endometrium. Reprod Sci, 2015. 22: 181–88
29. Kim MJ, Park SA, Kim CH et al: TGF-β type I receptor kinase inhibitor EW-7197 suppresses cholestatic liver fibrosis by inhibiting HIF1α-induced epithelial mesenchymal transition. Cell Physiol Biochem, 2016; 38: 571–88
30. Mendel I, Yacov N, Shoham A et al: Treatment with oxidized phospholipids directly inhibits nonalcoholic steatohepatitis and liver fibrosis without affecting steatosis. Dig Dis Sci, 2016; 61: 2545–53
31. Ankri-Eliahoo G, Weitz K, Cox TC, Tang GL: p27kip1 Knockout enhances collateralization in response to hind limb ischemia. J Vasc Surg, 2016; 63: 1351–59
32. Summers SA, Gan PY, Dewage L et al: Mast cell activation and degranulation promotes renal fibrosis in experimental unilateral ureteric obstruction. Kidney Int, 2012; 82: 676–85

Acknowledgements

This work received technical supported from the College of Pharmacy of Dalian Medical University and the Second Affiliated Hospital of Dalian Medical University, Dalian, Liaoning, China.

Conflict of interest

The authors declare that there are no financial or other relationships that might lead to a conflict of interest in the present article.

This work is licensed under Creative Common Attribution-NonCommercial-NoDerivatives 4.0 International (CC BY-NC-ND 4.0)

Indexed in: [Current Contents/Clinical Medicine] [SCI Expanded] [ISI Alerting System] [ISI Journals Master List] [Index Medicus/MEDLINE] [EMBASE/Excerpta Medica] [Chemical Abstracts/CAS] [Index Copernicus]